

Research

Open Access

Different forms of glycine- and GABA_A-receptor mediated inhibitory synaptic transmission in mouse superficial and deep dorsal horn neurons

Wayne B Anderson[†], Brett A Graham[†], Natalie J Beveridge, Paul A Tooney, Alan M Brichta and Robert J Callister*

Address: School of Biomedical Sciences and Pharmacy, The University of Newcastle and Hunter Medical Research Institute, University Drive, Callaghan, NSW 2308, Australia

Email: Wayne B Anderson - wayne.anderson@newcastle.edu.au; Brett A Graham - brett.graham@newcastle.edu.au;

Natalie J Beveridge - natalie.beveridge@newcastle.edu.au; Paul A Tooney - paul.tooney@newcastle.edu.au;

Alan M Brichta - alan.brichta@newcastle.edu.au; Robert J Callister* - robert.callister@newcastle.edu.au

* Corresponding author †Equal contributors

Published: 18 November 2009

Received: 31 May 2009

Molecular Pain 2009, **5**:65 doi:10.1186/1744-8069-5-65

Accepted: 18 November 2009

This article is available from: <http://www.molecularpain.com/content/5/1/65>

© 2009 Anderson et al; licensee BioMed Central Ltd.

This is an Open Access article distributed under the terms of the Creative Commons Attribution License (<http://creativecommons.org/licenses/by/2.0>), which permits unrestricted use, distribution, and reproduction in any medium, provided the original work is properly cited.

Abstract

Background: Neurons in superficial (SDH) and deep (DDH) laminae of the spinal cord dorsal horn receive sensory information from skin, muscle, joints and viscera. In both regions, glycine- (GlyR) and GABA_A-receptors (GABA_ARs) contribute to fast synaptic inhibition. For rat, several types of GABA_AR coexist in the two regions and each receptor type provides different contributions to inhibitory tone. Recent work in mouse has discovered an additional type of GlyR, (containing alpha 3 subunits) in the SDH. The contribution of differing forms of the GlyR to sensory processing in SDH and DDH is not understood.

Methods and Results: Here we compare fast inhibitory synaptic transmission in mouse (P17-37) SDH and DDH using patch-clamp electrophysiology in transverse spinal cord slices (L3-L5 segments, 23°C). GlyR-mediated mIPSCs were detected in 74% (25/34) and 94% (25/27) of SDH and DDH neurons, respectively. In contrast, GABA_AR-mediated mIPSCs were detected in virtually all neurons in both regions (93%, 14/15 and 100%, 18/18). Several Gly- and GABA_AR properties also differed in SDH vs. DDH. GlyR-mediated mIPSC amplitude was smaller (37.1 ± 3.9 vs. 64.7 ± 5.0 pA; $n = 25$ each), decay time was slower (8.5 ± 0.8 vs. 5.5 ± 0.3 ms), and frequency was lower (0.15 ± 0.03 vs. 0.72 ± 0.13 Hz) in SDH vs. DDH neurons. In contrast, GABA_AR-mediated mIPSCs had similar amplitudes (25.6 ± 2.4 , $n = 14$ vs. $25. \pm 2.0$ pA, $n = 18$) and frequencies (0.21 ± 0.08 vs. 0.18 ± 0.04 Hz) in both regions; however, decay times were slower (23.0 ± 3.2 vs. 18.9 ± 1.8 ms) in SDH neurons. Mean single channel conductance underlying mIPSCs was identical for GlyRs (54.3 ± 1.6 pS, $n = 11$ vs. 55.7 ± 1.8 , $n = 8$) and GABA_ARs (22.7 ± 1.7 pS, $n = 10$ vs. 22.4 ± 2.0 pS, $n = 11$) in both regions. We also tested whether the synthetic endocannabinoid, methandamide (methAEA), had direct effects on Gly- and GABA_ARs in each spinal cord region. MethAEA (5 μM) reduced GlyR-mediated mIPSC frequency in SDH and DDH, but did not affect other properties. Similar results were observed for GABA_AR mediated mIPSCs, however, rise time was slowed by methAEA in SDH neurons.

Conclusion: Together these data show that Gly- and GABA_ARs with clearly differing physiological properties and cannabinoid-sensitivity contribute to fast synaptic inhibition in mouse SDH and DDH.

Background

The superficial and deep laminae of the spinal cord dorsal horn, termed SDH and DDH respectively, are important sites for processing sensory information arising in skin, muscle, joints and viscera [1,2]. This information arrives in the dorsal horn via primary afferents, which have specific termination patterns in SDH (laminae I-II) and DDH (laminae IV-VI) depending on their axon diameter, sensory modality and peripheral origin [3-5]. The SDH receives inputs predominately from small diameter A δ and C-fibres carrying nociceptive, thermal, itch, and innocuous tactile information [6-11]. In contrast, the DDH receives inputs predominately from larger A β myelinated fibres carrying tactile information [3,12,13].

As with primary afferent inputs, the outputs of the SDH and DDH, which are conveyed by projection neurons, also differ. Projections from the SDH terminate mostly in brainstem and midbrain centres such as the parabrachial nuclei and periaqueductal grey [14,15]. In contrast, projections from the DDH terminate mainly in the thalamus [16,17]. Recent evidence also suggests intrinsic synaptic connectivity differs in the two regions. For example, paired recordings in SDH neurons show a modular pattern of synaptic linkages connecting a restricted number of neuron types [18,19]. Similar recordings in the DDH suggest a more extensive synaptic connectivity among neuron classes [20].

These recent data suggest synaptic processing mechanisms differ in the SDH and DDH. Indeed, some aspects of fast inhibitory synaptic transmission, mediated by GABA_A and glycine receptors (GlyRs) differ in the SDH and DDH. For example, c-Fos expression differs in the SDH and DDH after blockade of tonic inhibition with specific GABA_A and GlyR antagonists [21] and an unusual form of the GlyR, containing alpha 3-subunits, is confined to the SDH of the mouse spinal cord [22]. These data suggest the two receptors play differing roles in setting inhibitory tone and subsequent processing of sensory information in the two regions.

The type-one cannabinoid receptor (CB₁R), which has long been known to be involved in analgesia [23,24], is also expressed at different levels in the SDH versus DDH [25]. The CB₁R appears to be more highly expressed in the SDH, consistent with the analgesic action of cannabinoids. Several mechanisms have been proposed for the analgesic action of cannabinoids including modulation of glutamatergic [26,27], noradrenergic [28] and opioidergic

systems [29,30]. In addition to these CB₁R mediated effects, several reports have suggested cannabinoids also act directly on GlyRs [31,32]. One study reported attenuation of glycinergic currents by cannabinoids in isolated hippocampal and Purkinje neurons [32], whereas another has reported cannabinoids potentiate glycine-activated currents in isolated ventral tegmental area neurons and in recombinant GlyRs [31]. No studies have investigated the effects of cannabinoids on "native", synaptically located GlyRs on SDH or DDH neurons.

In this paper, we first characterize synaptically-mediated miniature inhibitory postsynaptic currents (mIPSCs) in both the SDH and DDH of the mouse spinal cord using patch clamp techniques. We then test whether the synthetic endocannabinoid, methanadamide (methAEA), has direct effects on synaptically located Gly- and GABA_ARs in the SDH and DDH. Finally, we use real-time PCR (qPCR) to quantify and compare subunit expression of Gly- and GABA_ARs, and the CB₁R in the SDH and DDH.

Methods

Tissue preparation

All experimental procedures were approved by the University of Newcastle Animal Care and Ethics Committee. Mice (C57/Bl6; both sexes, aged 17-37 days) were anaesthetized with Ketamine (100 mg kg⁻¹ i.p.) and decapitated. The vertebral column (~T5 - S1) was isolated and immersed in ice-cold oxygenated sucrose substituted artificial cerebro-spinal fluid (S-ACSF). This solution contained (in mM): 250 sucrose, 25 NaHCO₃, 10 glucose, 2.5 KCl, 1 NaH₂PO₄, 1 MgCl₂ and 2.5 CaCl₂ and was bubbled with Carbogen (95% O₂ and 5% CO₂). The lumbar spinal cord (L1 - L6) was removed, placed against a Styrofoam support block, and glued (rostral side down) to a cutting platform with cyanoacrylate glue (Loctite 454, Loctite, Caringbah, Australia). The cutting platform was then transferred to a cutting chamber, filled with ice-cold S-ACSF, and transverse slices (300 μ m-thick) were obtained from the L3-L5 segments using a vibratome (Leica Microsystems, Wetzlar, Germany). Slices were transferred to a storage chamber containing Carbogen-bubbled artificial cerebro-spinal fluid (ACSF; 118 mM NaCl substituted for sucrose in S-ACSF) and allowed to equilibrate for 1 h before electrophysiological recording.

Electrophysiology

Individual slices were transferred to a recording chamber (bath volume 0.4 ml) and continually perfused (exchange rate 4-6 bath volumes/min) with bubbled ACSF. Neurons

were visualized in spinal cord slices using infrared differential interference contrast optics (IR-DIC) and a Hamamatsu charge coupled device camera (Model C-2400-79H, Hamamatsu City, Japan) linked to a video monitor. Under IR-DIC lamina II appears as a translucent band that clearly delineates the lamina II-III border in mice older than six days (P6) [33]. All SDH recordings were made between this border and the dorsal white matter. We defined the DDH as the grey matter dorsal to the central canal, and more than 100 μm ventral to lamina II. All our DDH recordings were made within these boundaries. Patch pipettes (3-4 M Ω resistance), made from borosilicate glass (1.5 mm O.D; PG150T-15; Harvard Apparatus, UK) were filled with an internal solution containing (in mM): 130 CsCl, 10 HEPES, 10 EGTA, 1 MgCl₂, 2 ATP and 0.3 GTP (pH adjusted to 7.35 with 1 M CsOH). Under these recording conditions the reversal potential for chloride ions is 0 mV: thus, at a holding potential of -70 mV all chloride-mediated inhibitory currents are inward. Whole-cell voltage-clamp recordings were made at room temperature (22 - 24 °C) from SDH and DDH neurons. After obtaining the whole-cell recording configuration, series resistance and neuronal input resistance were assessed according to the response to a 5 mV hyperpolarizing step (average of 20 repetitions, holding potential -70 mV). These values were monitored at the beginning and end of each recording session, and data were rejected if values changed by > 20%. Series resistance (< 20 M Ω) was uncompensated in all experiments. All synaptic currents were recorded at a holding potential of -70 mV using an Axopatch 200B amplifier (Molecular Devices, Sunnyvale, CA, USA). Signals were filtered at 2 kHz and digitized online at 10 kHz via an Instrutech ITC-16i A/D board (Instrutech, Long Island, NY, USA). Data were stored on a Macintosh G4 computer and analysed offline using Axograph v4.6 software (Molecular Devices, Sunnyvale, CA, USA).

Experimental protocols

mIPSCs, which are considered to be the postsynaptic response to the spontaneous release of single vesicles of neurotransmitter [34], were recorded as follows. GlyR-mediated mIPSCs were pharmacologically isolated by bath application of the AMPA-kainate receptor antagonist 6-cyano-7-nitroquinoxaline-2,3-dione (CNQX; 10 μM), the GABA_A receptor antagonist bicuculline (10 μM), and the sodium channel blocker tetrodotoxin (TTX; 1 μM). Data collection commenced 3 minutes after drugs were washed into the recording bath (wash-on) and continued for at least another 3 minutes. These mIPSCs were completely abolished by subsequent bath application of the GlyR antagonist strychnine (1 μM ; n = 10). GABA_AR-mediated mIPSCs were pharmacologically isolated in CNQX (10 μM), strychnine (1 μM), and TTX (1 μM), and were abolished by bath application of bicuculline (10 μM ;

n = 10). The effect of the synthetic endocannabinoid, methAEA (5 μM), on GlyR- and GABA_AR-mediated mIPSCs was tested in a subset of neurons where mIPSC frequency was relatively high (> 1 Hz). MethAEA was allowed to wash-on for at least 10 minutes before mIPSCs were recorded for analysis. Each recorded neuron's location was carefully noted and mapped as described previously at the completion of each recording session [35]. The templates for L3, L4, and L5 spinal cord segments (Figure 1) were adapted from Franklin and Paxinos' Mouse Brain Atlas [36].

Analysis of mIPSC properties

Pharmacologically isolated GlyR- and GABA_AR-mediated mIPSCs were detected and captured using a sliding template method (semi-automated procedure within Axograph software package [37]). Captured mIPSCs were inspected individually and accepted for analysis when: (1) the captured trace did not contain overlapping mIPSCs; (2) the baseline before the rise, or after the decay phase of the mIPSC trace was stable for > 5 ms; and (3) no time-dependent trend was evident in either mIPSC amplitude or instantaneous frequency over the recording period [38]. Analyses were performed on averaged mIPSCs, obtained by aligning the rising phase of all accepted mIPSCs for a given neuron. Peak amplitude, rise time (calculated over 10-90% of peak amplitude), and decay time constant (calculated over 20-80% of the decay phase) were calculated using semi-automated procedures within Axograph software. In both SDH and DDH neurons, GlyR- and GABA_AR-mediated mIPSCs were best fit by a single decay time constant [39].

Analysis of single channel conductance

The single-channel conductance underlying mIPSCs was determined by peak scaled nonstationary noise analysis [40] using the Mini Analysis Program (v6; Synaptosoft, Fort Lee, NJ, USA). This procedure calculates a weighted mean of the underlying multiple conductance states for synaptically located receptors, that is, those generating the recorded mIPSCs versus receptors located outside the synaptic cleft. Briefly, for each neuron, mIPSCs were aligned at the midpoint of their rising phase and averaged. This averaged mIPSC was then scaled to the peak amplitude of all captured mIPSCs that contributed to the averaged mIPSC. The peak scaled average current was then subtracted from individual (scaled) mIPSCs to obtain a difference current, which represents random receptor fluctuations around the mean. Difference currents were binned over the decay phase of the mIPSC. The variance was then plotted against the mean current. A parabolic function (variance = $I [\text{current}] - [\text{current}^2]/N^P + \text{baseline noise}$) was then fit to the variance/mean plot, where I is single-channel current, N is the average number of channels open at mIPSC peak, and P is open probability [40].

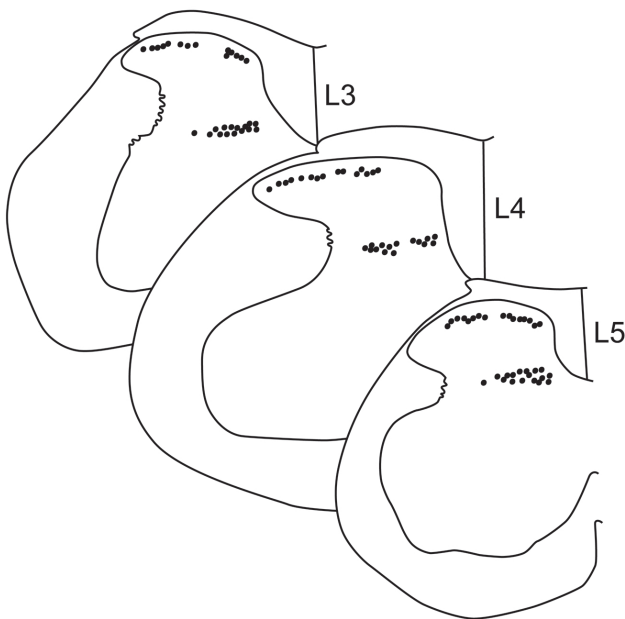


Figure 1
Location of recorded SDH and DDH neurons in lumbo-sacral spinal cord. The location of each recorded neuron was plotted on templates of the L3, L4, and L5 spinal cord segments. Approximately 30 neurons were recorded in each segment. For SDH neurons, recordings were obtained across the entire medio-lateral extent of the dorsal horn. For DDH neurons, recordings were concentrated in the medial two thirds of the dorsal horn because dense myelination impedes visualizing neurons in lateral DDH.

RNA extraction and relative real-time PCR

A separate set of experiments were undertaken to quantify Gly-, GABA_AR and CB₁R subunit mRNA. Spinal cord slices were prepared as described above and each slice was microdissected into 2 regions containing the SDH and DDH. This procedure yielded two pieces of tissue per slice. The SDH and DDH regions for all slices (six slices, L3 - L5) were pooled by region, and prepared for relative real-time PCR (qPCR). Total RNA was extracted from the tissue using TRIzol reagent (Invitrogen, USA) [41]. Tissue was added to TRIzol reagent and total RNA was prepared according to the manufacturer's instructions. RNA integrity was assessed by A260/A280 ratios (> 1.8), or visualisation of 18s and 28s ribosomal bands by electrophoresis with formaldehyde denaturing 1% agarose gel. Total RNA was treated with DNase1 (Invitrogen, USA) and reverse transcribed with SuperscriptII reverse transcriptase (Invitrogen, USA) as per manufacturer's instructions. Real-time PCR using SYBR Green PCR Mastermix (PE Applied Biosystems, UK) and an ABI prism 7500 sequence detection system (PE Applied Biosystems, UK) was performed to assess the expression of the GlyR subunit genes (α 1-4 and

β), GABA_AR subunit genes (α 1- α 3, α 5, β 2-3, γ 2) and CB₁R levels. Primers (Additional File 1) were designed for each gene using Primer Premier 5.0 (Premier Biosoft International, USA). Reactions consisting of 2 × SYBR Green PCR Mastermix, 40 nM of each primer, cDNA template, and nuclease-free water were run in triplicate for each gene on the ABI 7500 sequence detection system under the following conditions: 50°C for 2 min, 95°C for 10 min, 45 cycles of 95°C for 15 s and 60°C for 90 s. Dissociation curves consisting of 95°C for 15 s and 60°C for 15 s, followed by a 2% ramp to 95°C were used to ensure a single product of the correct molecular size was present in each reaction. An average cycle threshold value (Ct) was calculated from triplicate results for each gene. Threshold values were normalized to the housekeeping gene β -actin to provide Δ Ct values. Relative expression levels for each gene were then calculated using the formula $2^{-\Delta\text{Ct}}$. Finally, we calculated a ratio for all GlyR- and GABA_AR- subunits in a given sample (eg, GlyR α 1: α 2) and then compared the average ratios between the SDH and DDH.

Statistical analysis

SPSS v13 software package (SPSS Inc. IL, USA) was used for all statistical analyses. Student's unpaired t-tests were used to compare mIPSC properties recorded in the SDH and DDH, and to compare mIPSC properties before and after exposure to methAEA. One-way ANOVA's compared gene expression data for all GlyR- and GABA_AR subunits in the SDH and DDH. Student's unpaired t-tests compared gene expression for each subunit (GlyR, GABA_AR and CB₁) in the SDH versus DDH. When data were not normally distributed non-parametric statistics (Mann-Whitney two sample tests) were applied. All values are presented as means \pm SEM. Statistical significance was set at $p < 0.05$.

Drugs

TTX was obtained from Alomone Laboratories (Jerusalem, Israel), and methAEA from Tocris Bioscience (Bristol, UK). All other drugs were purchased from Sigma Chemicals (St Louis, MO, USA).

Results

Whole-cell patch clamp recordings were obtained from 92 neurons in 18 animals in either the SDH ($n = 45$) or the DDH ($n = 47$) as illustrated in Figure 1. Mean animal age (21.4 ± 0.3 vs. 21.9 ± 0.3 days) and series resistance (11.6 ± 0.7 vs. 11.6 ± 0.6 M Ω) were similar for SDH and DDH recordings, suggesting neither age nor recording conditions influenced our results. In contrast, input resistance was higher in SDH neurons (640 ± 65 vs. 260 ± 30 M Ω). This is consistent with morphology data, which shows SDH neurons are smaller than those in the DDH [42,43]. GlyR-mediated mIPSCs were detected in 74% (25/34) of SDH neurons and in almost all DDH neurons (93%; 25/

27). In contrast, GABA_AR-mediated mIPSCs were detected in virtually all neurons in our dorsal horn recordings: 93% (14/15) and 100% (18/18) for SDH and DDH neurons, respectively. Thus, inhibitory synaptic transmission at GlyR-containing synapses is more prominent in the DDH, whereas GABA_AR-containing synapses are distributed similarly in both regions of the mouse spinal cord dorsal horn.

Glycine receptor-mediated synaptic transmission

Figure 2 and Table 1 compare the properties of GlyR-mediated mIPSCs recorded in SDH and DDH neurons. Mean mIPSC amplitude in SDH neurons was approximately half that observed in DDH neurons (37.1 ± 3.9 vs. 64.7 ± 5.0 pA, $n = 25$ and $n = 25$ respectively; Figure 2A & 2C). mIPSC kinetics also differed between the two regions. The decay time constant for mIPSCs was slower in SDH versus DDH neurons (8.5 ± 0.8 vs. 5.5 ± 0.3 ms), however, mIPSC rise times were identical in the two regions (0.85 ± 0.07 vs. 0.85 ± 0.04 ms). mIPSC frequency was lower in the SDH compared to the DDH (0.15 ± 0.03 vs. 0.72 ± 0.13 Hz). Interestingly, the combined effect of smaller slow decaying mIPSCs in the SDH and larger fast decaying mIPSCs in the DDH resulted in a similar charge transfer per mIPSC in the two regions (364.5 ± 57.7 vs. 456.6 ± 39.9 pA.ms). However, when glycinergic charge is multiplied by mIPSC frequency, to provide an overall measure of glycinergic drive, the result is a more than seven fold greater drive in DDH versus SDH (68.0 ± 26.8 vs. 400.0 ± 107.9 pA.ms.Hz). Of course under in vivo conditions neurotransmitter release is driven largely by action potential invasion of presynaptic terminals. Thus, in vivo differences in background discharge (not assessed in this study) will contribute to overall levels of glycinergic drive in the two regions.

The marked differences in GlyR-mediated mIPSC amplitude in SDH and DDH neurons could be attributable to specific properties of the GlyR, such as differences in single-channel conductance, number of receptors open during quantal release (N_o), or channel open probability (P_o). To distinguish between these possibilities, peak-scaled nonstationary noise analysis was undertaken on a subset of mIPSC recordings from SDH and DDH neurons (Table 1). This analysis showed both unitary conductance (54.3 ± 1.6 vs. 55.7 ± 1.8 pS, $n = 8$ and $n = 11$, respectively) and P_o (0.97 ± 0.01 vs. 0.99 ± 0.01), were identical for GlyRs in the SDH and DDH, however, only half the number of channels (10.3 ± 0.5 vs. 19.0 ± 5.3) contributed to mean quantal current in the SDH versus DDH.

GABA_A receptor-mediated synaptic transmission

Many of the properties of GABA_AR-mediated mIPSCs were similar in SDH and DDH neurons (Table 1, Figure 3). Specifically, mIPSC amplitude (25.6 ± 2.4 vs. 25.3 ± 2.0

pA, $n = 14$ and $n = 18$, respectively) and frequency (0.21 ± 0.08 vs. 0.18 ± 0.04 Hz) were similar in both regions (Figure 3A & 3C). The rise time and decay time constant of GABA_AR-mediated mIPSCs, however, was significantly slower in the SDH (1.97 ± 0.18 vs. 1.49 ± 0.10 ms, and 23.0 ± 3.2 vs. 18.9 ± 1.6 ms). Interestingly, the slower decay times of GABA_A-mediated mIPSCs in the SDH resulted in a significantly greater charge transfer per mIPSC in SDH versus DDH neurons (717.3 ± 75.5 vs. 486.3 ± 52.4 pA.ms). GABA_AR-mediated drive, as estimated by measuring mIPSC charge transfer by event frequency, however, was similar in both regions (152.4 ± 61.9 vs. 92.8 ± 21.1 pA.ms.Hz).

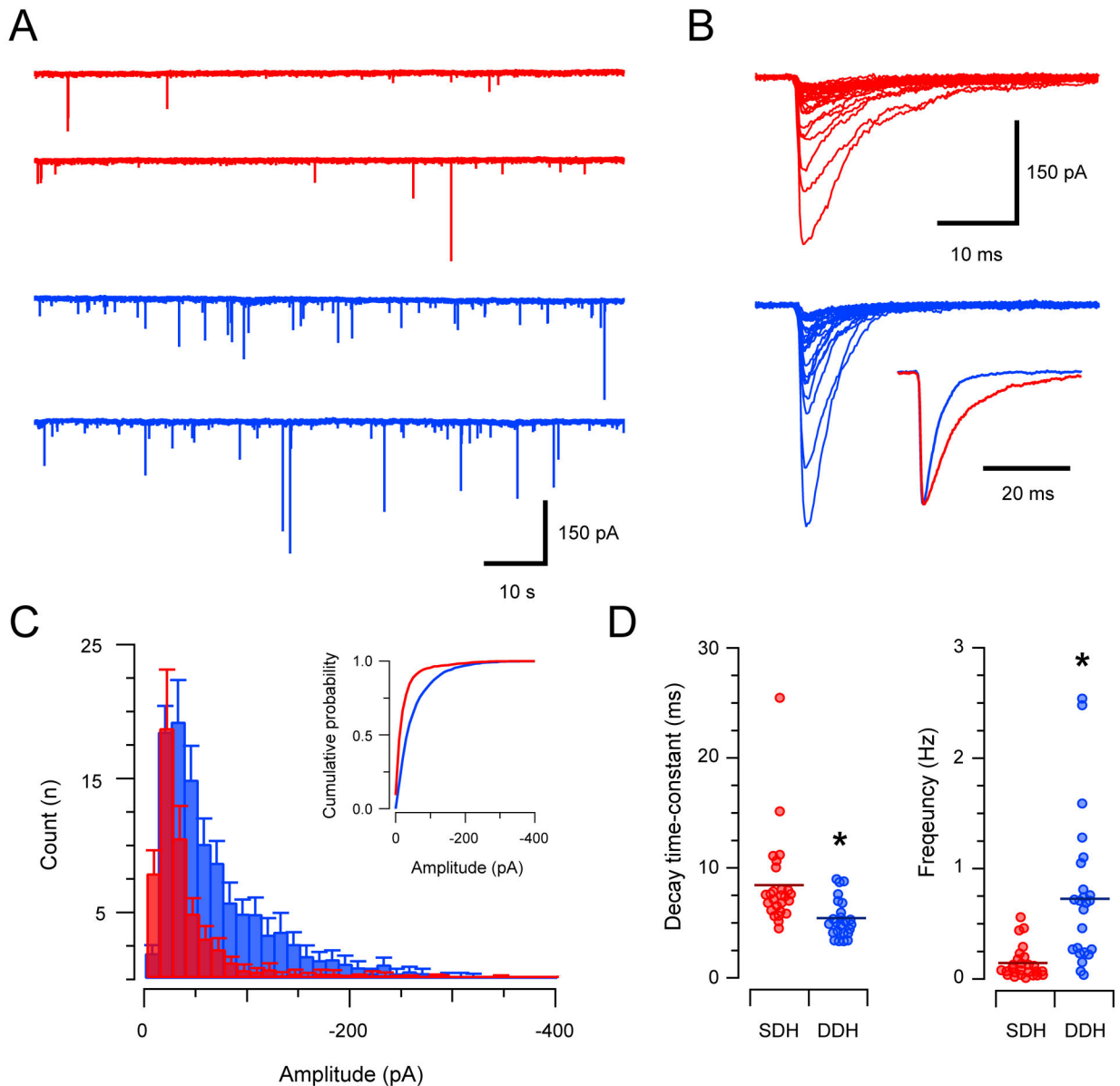
Peak-scaled nonstationary noise analysis was also applied to GABA_AR-mediated mIPSCs to examine the properties of synaptically located receptors. This analysis showed that GABA_ARs underlying the mIPSCs had an identical unitary conductance in the SDH and DDH (22.7 ± 1.7 vs. 22.4 ± 2.0 pS, $n = 8$ and $n = 11$, respectively). P_o was lower in SDH neurons (0.76 ± 0.04 vs. 0.94 ± 0.02) and N_o was greater in SDH neurons (18.5 ± 1.6 vs. 12.9 ± 1.0). These data suggest more GABA_A channels underlie quantal transmission in the SDH but open probability is lower.

Cannabinoid effects on GlyR-mediated synaptic transmission

Two studies have suggested that cannabinoids have *direct* (allosteric) effects on recombinant or cultured GlyRs [31,44]. To test for direct cannabinoid effects on native GlyRs in the SDH or DDH we compared the properties of GlyR-mediated mIPSCs, recorded in both regions, before and after bath application of the synthetic endocannabinoid, methAEA ($5 \mu\text{M}$). Figure 4A shows the effect of methAEA on glycinergic mIPSCs in the SDH. MethAEA significantly reduced mIPSC frequency (0.18 ± 0.03 vs. 0.08 ± 0.02 Hz, $n = 7$). In contrast, methAEA had no effect on mIPSC amplitude (35.9 ± 5.7 vs. 31.7 ± 3.4 pA), rise time (0.81 ± 0.16 vs. 0.96 ± 0.08 ms), or decay time constant (7.86 ± 1.10 vs. 7.93 ± 1.03 ms). Figure 4B summarizes the effect of methAEA on GlyR-mediated mIPSCs in the DDH. As in the SDH, methAEA significantly reduced GlyR-mediated mIPSC frequency (0.37 ± 0.09 vs. 0.15 ± 0.03 Hz, $n = 8$) in DDH neurons. MethAEA, however, did not affect mIPSC amplitude (62.4 ± 6.0 vs. 52.2 ± 6.8 pA), rise time (0.63 ± 0.03 vs. 0.60 ± 0.09 ms), or decay time constant (5.04 ± 0.68 vs. 5.02 ± 0.57 ms). In summary, methAEA reduced mIPSC frequency but had no direct effect on GlyRs located at synapses on either SDH or DDH neurons.

Cannabinoid effects on GABA_AR-mediated synaptic transmission

We next tested if methAEA had direct effects on GABA_AR-mediated mIPSCs in the SDH or DDH. Figure 5A summa-

**Figure 2**

GlyR-mediated synaptic transmission in the SDH and DDH. **A** representative traces showing continuous recordings of GlyR-mediated mIPSCs (holding potential -70 mV) in the presence of TTX (1 μ M), CNQX (10 μ M), and bicuculline (10 μ M) from an SDH (red traces) and a DDH neuron (blue traces). Note mIPSC frequency is considerably higher in DDH neurons. **B** individual mIPSCs from traces in A (aligned at rise onset) showing the amplitude variability in GlyR-mediated mIPSCs recorded in both the SDH (red traces) and DDH (blue traces). Inset shows averaged mIPSCs normalised to the same amplitude (same neurons in A). Note the slower decay time of GlyR-mediated mIPSCs in SDH neurons. **C** overlaid histograms comparing amplitude distributions of GlyR-mediated mIPSCs in SDH (red) and DDH (blue) neurons (n = 25 neurons for SDH and DDH). In the SDH distribution, only 10% of mIPSCs have amplitudes greater than 50 pA, whereas 35% of the mIPSCs in the DDH distribution are greater than 50 pA. Inset shows data presented as cumulative probability plots. **D** plots comparing group data for GlyR-mediated mIPSC decay time-constant and frequency in SDH and DDH neurons. GlyR-mediated mIPSC decay time-constants were slower and mIPSC frequency was lower in SDH neurons.

Table 1: Properties of mIPSCs in mouse SDH and DDH neurons

mIPSC type	Region	mIPSC properties						Channel properties			
		Amplitude (pA)	Rise time (ms)	Decay time (ms)	Frequency (Hz)	Charge ^δ (pA.ms)	n	Conductance (pS)	Open probability (P _o)	Channel number	n
Glycine	SDH	37.1 ± 3.9*	0.85 ± 0.07	8.5 ± 0.8*	0.15 ± 0.03*	364.5 ± 57.7	25	54.3 ± 1.6	.97 ± 0.01	10.3 ± 0.5*	8
	DDH	64.7 ± 5.0	0.85 ± 0.04	5.5 ± 0.3	0.72 ± 0.13	456.6 ± 39.9	25	55.7 ± 1.8	.99 ± 0.01	19.0 ± 5.3	11
GABA _A	SDH	25.6 ± 2.4	1.97 ± 0.18*	23.0 ± 3.2*	0.21 ± 0.08	717.3 ± 75.5*	14	22.7 ± 1.7	0.76 ± 0.04*	18.5 ± 1.6*	8
	DDH	25.3 ± 2.0	1.49 ± 0.10	18.9 ± 1.6	0.18 ± 0.04	486.3 ± 52.4	18	22.4 ± 2.0	0.94 ± 0.02	12.9 ± 1.0	11

* indicates significant differences for SDH and DDH values

^δ mIPSC charge calculated in Axograph using averages for peak amplitude, rise- and decay times

rises the effect of methAEA on GABA_Aergic synaptic transmission in SDH neurons. MethAEA produced a significant reduction in mIPSC frequency (0.27 ± 0.05 vs. 0.18 ± 0.03 Hz, $n = 6$), without altering mIPSC amplitude (30.1 ± 1.7 vs. 28.1 ± 0.9 pA), or decay time constant (29.51 ± 7.39 vs. 37.52 ± 12.57 ms). The rise time of GABA_Aergic mIPSCs, however, was slowed by methAEA (1.89 ± 0.52 vs. 2.51 ± 0.69 ms). Figure 5B summarises the effect of methAEA on GABA_AR-mediated mIPSCs in DDH neurons. Bath application of methAEA significantly reduced mIPSC frequency (0.20 ± 0.04 vs. 0.05 ± 0.02 Hz, $n = 7$), but did not affect mIPSC amplitude (19.6 ± 1.3 vs. 17.0 ± 1.1 pA), rise time (1.58 ± 0.17 vs. 2.10 ± 0.51 ms), or decay time constant (19.70 ± 3.52 vs. 23.10 ± 4.64 ms). These results suggest the predominant effect of methAEA is to reduce GABA_AR-mediated mIPSC frequency, though the slowed rise times suggest a postsynaptic effect of methAEA, possibly involving a direct interaction on GABA_ARs.

Expression of glycine, GABA_A, and CB₁ receptor subunits in SDH and DDH

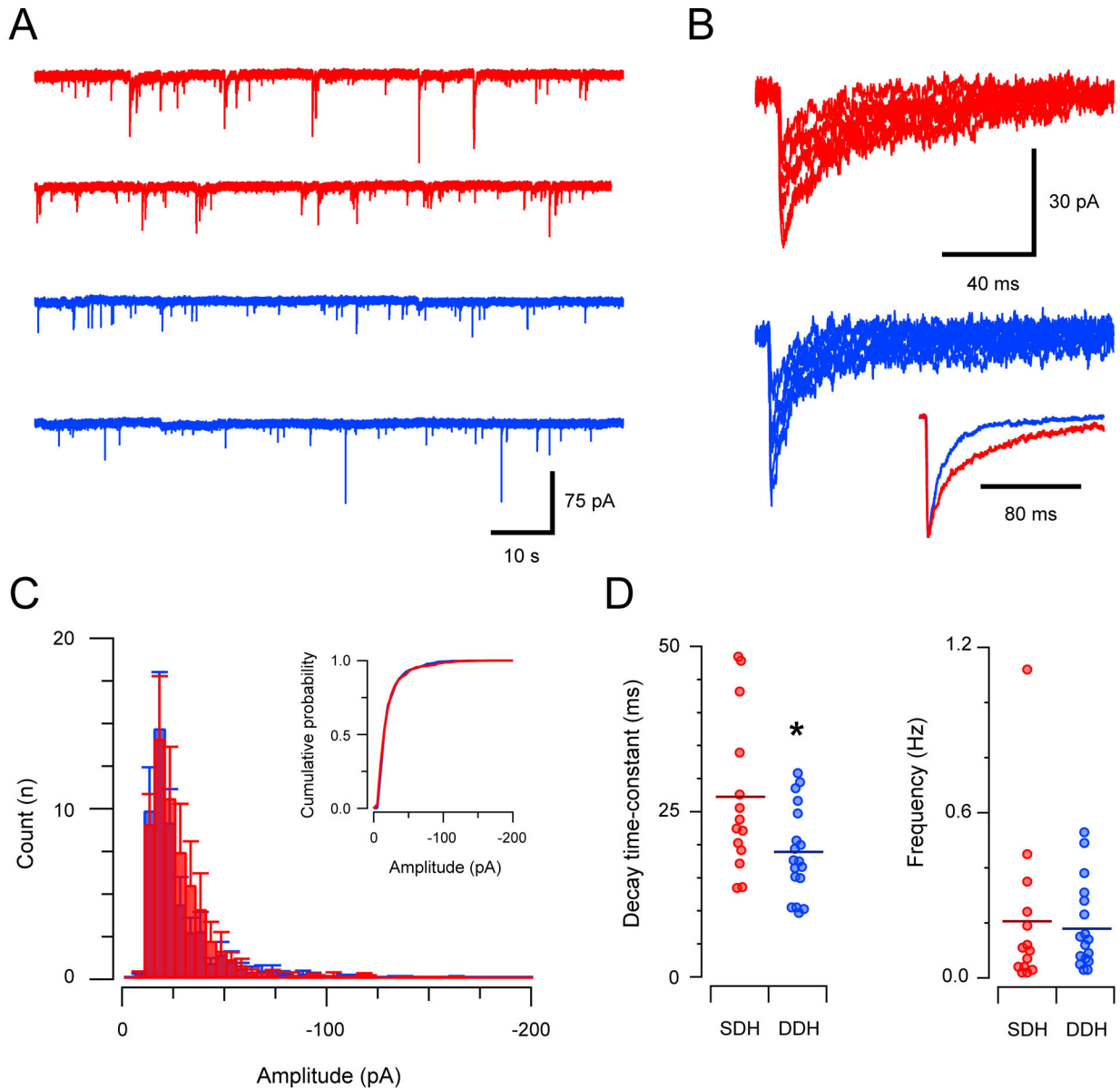
Because GlyR- and GABA_AR-mediated mIPSC properties differ markedly in SDH and DDH neurons, we next analysed subunit expression of both receptors in each region using qPCR. Figure 6 summarises qPCR results for Gly- and GABA_AR subunits in the SDH and DDH. Data are presented as relative expression values. In the SDH (Figure 6A, left) Gly α 1 is most highly expressed, followed by Gly β , Gly α 3 and Gly α 2, with negligible expression of Gly α 4. In the DDH (Figure 6A, right), Gly α 1 is again the most highly expressed subunit, followed by Gly β . Gly α 2, Gly α 3, and Gly α 4 are expressed at much lower levels. Comparison of each GlyR subunit in SDH versus DDH showed Gly α 1, Gly α 2, Gly α 4 and Gly β were more highly expressed in the DDH (Figure 6A). The results of GABA_AR subunit expression in the SDH (Figure 6B, left) showed no significant differences in subunit expression. In the DDH (Figure 6B, right), qPCR analysis also failed to resolve any differences in GABA_AR subunit expression. Comparison of each GABA_AR subunit in SDH versus DDH shows that only expression levels of GABA α 1 and GABA β 2 differed in

the two regions. Again higher expression levels were detected in the DDH. Finally, comparison of CB₁R relative expression using qPCR in the SDH and DDH detected significantly higher relative expression in the DDH (0.007 ± 0.001 vs. 0.025 ± 0.006 , respectively).

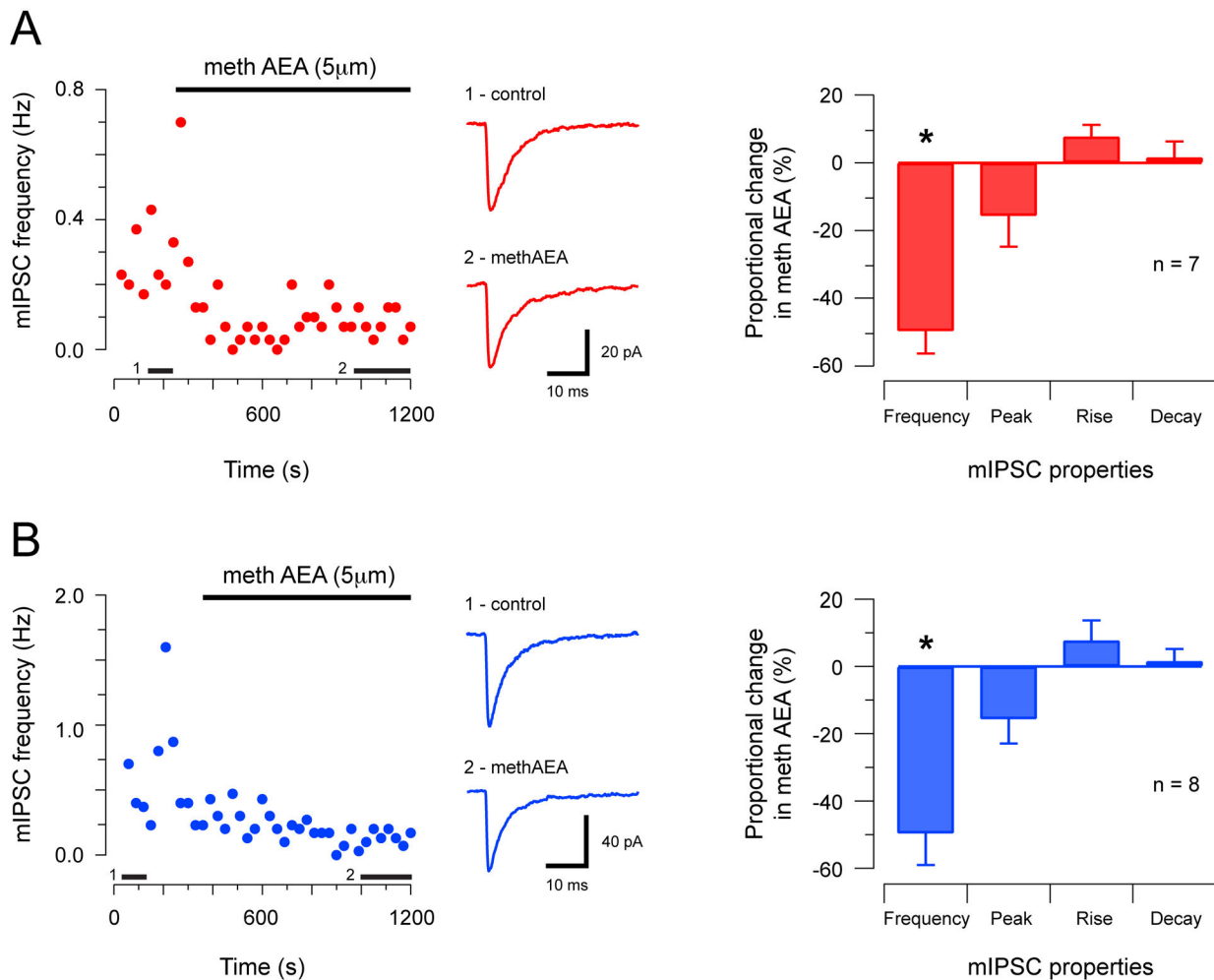
Because both GlyR and GABA_ARs are heteropentamers at native synapses we further analyzed all possible subunit combinations for both receptor types in the SDH and DDH. Comparisons for GlyR subunit combinations are presented in Table 2. This analysis showed possible subunit combinations are differentially weighted in the two regions. For example, the Gly α 1:Gly α 2 ratio is higher in the SDH, whereas the Gly α 1:Gly α 3 ratio is higher in the DDH. This finding suggests an increased likelihood of Gly α 1:Gly α 2 combinations in the DDH and that Gly α 1:Gly α 3 combinations would be more prevalent in the SDH. A similar analysis was conducted for GABA_AR subunits and none of the possible comparisons were significantly different (data not shown).

Discussion

We found the properties of GlyR- and GABA_A-mediated mIPSCs to be clearly different in SDH and DDH, suggesting the contribution of each receptor type to fast synaptic inhibition differs between the two regions. An additional aim of our experiments was to examine the action of an endocannabinoid on the two ligand-gated ion channels that are important for inhibitory signalling in the dorsal horn of the spinal cord. Our experiments were driven by three considerations: both Gly- and GABA_ARs have been implicated in the onset and maintenance of various pain states; the existence of a unique type of GlyR, containing α 3 subunits in the SDH of the mouse spinal cord; and reports of a direct (allosteric) action of cannabinoids on GlyRs in oocytes and dissociated neurons. We found no evidence for a 'direct effect' of methAEA on GlyR function in either the SDH or DDH. The rise time of GABA_AR-mediated mIPSCs, however, was slowed by methAEA in SDH neurons, suggesting a direct effect on GABA_AR-mediated mIPSCs. Our real-time PCR data showed the balance of

**Figure 3**

GABA_AR-mediated synaptic transmission in the SDH and DDH. **A** representative traces showing continuous recordings of GABA_AR-mediated mIPSCs (holding potential -70 mV) in the presence of TTX (1 μM), CNQX (10 μM), and strychnine (1 μM) from an SDH (red traces) and a DDH neuron (blue traces). Note similar mIPSC frequency in the neurons from the two regions. **B** individual mIPSCs from traces in A (aligned at rise onset) showing amplitude variability of GABA_AR-mediated mIPSCs in both SDH (red traces) and DDH (blue traces). Inset shows averaged mIPSCs normalised to the same amplitude (same neurons as in A). Note the slower decay time of GABA_AR-mediated mIPSCs in SDH neurons. **C** overlaid group data histograms comparing amplitude distributions for GABA_Aergic mIPSCs in SDH (red) and DDH (blue) neurons (n = 14 and 18 for SDH and DDH, respectively). The overlap of the two distributions indicates that GABA_AR-mediated mIPSC amplitudes are similar in SDH and DDH neurons. Inset shows data presented as cumulative distribution plots. **D** plots comparing group data for GABA_AR-mediated mIPSC decay time-constant and frequency in SDH and DDH neurons. GABA_AR-mediated mIPSC decay time-constants were significantly slower in SDH neurons, however, mIPSC frequency was similar in both regions.

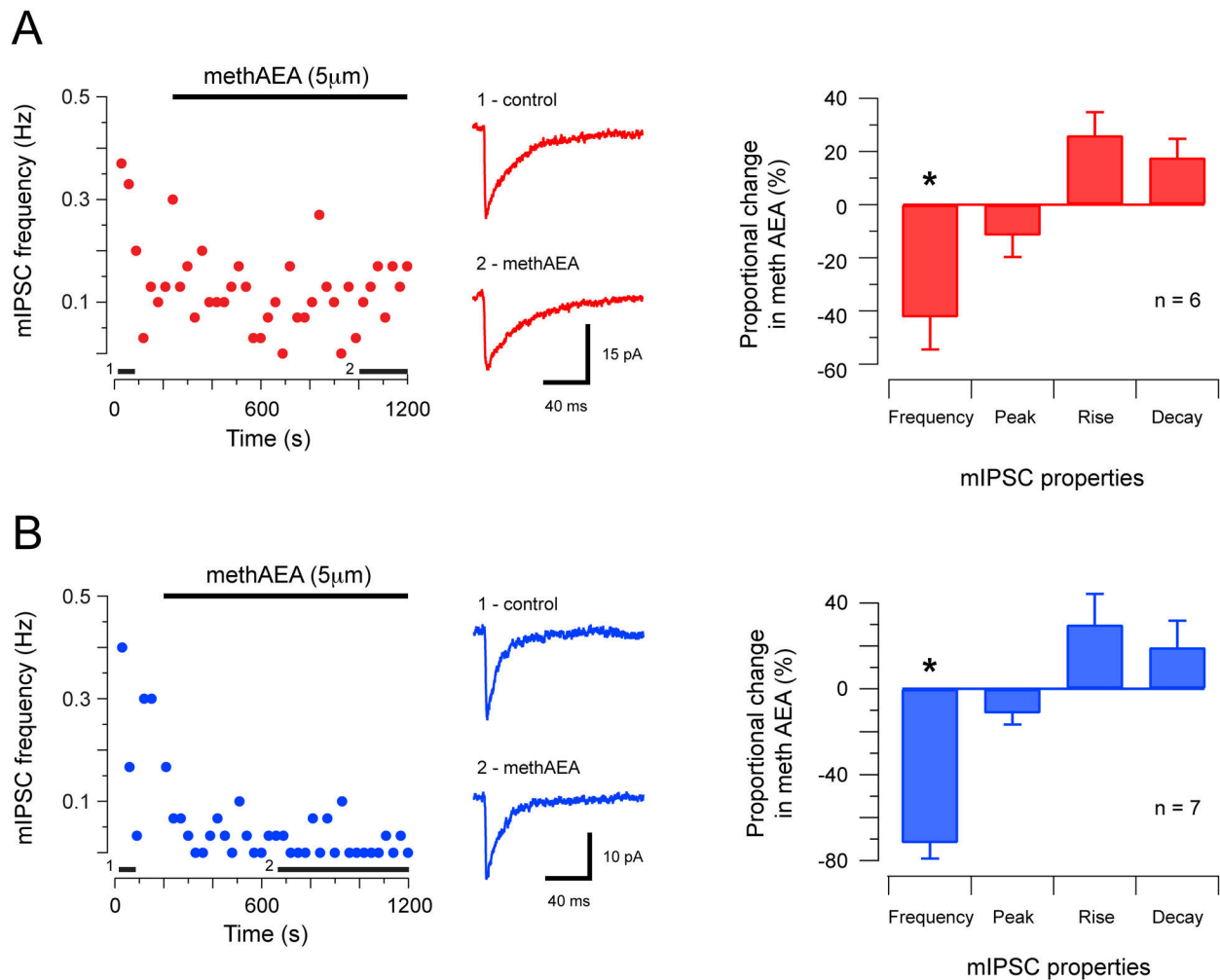
**Figure 4**

Effect of methanandamide on GlyR-mediated synaptic transmission in SDH and DDH neurons. **A** plot showing GlyR-mediated mIPSC frequency (holding potential -70 mV) in an SDH neuron during bath application of methAEA (5 μ m, upper bar). mIPSC frequency declines in the presence of methAEA. Middle traces are averaged mIPSCs ($n = 15$) under control conditions, and after 10 minutes in methAEA. Black bars above x-axis indicate when averaged mIPSCs were obtained. Plot on right presents group data summarising proportional changes in GlyR-mediated mIPSC properties in methAEA. mIPSC frequency was reduced in methAEA. mIPSC peak amplitude, rise time, and decay time-constant were unaltered. **B** Effect of methAEA on GlyR-mediated mIPSCs in DDH neurons (data presented in same format as A). methAEA also reduced GlyR-mediated mIPSC frequency in DDH neurons without altering mIPSC peak amplitude, rise time, or decay time-constant. Note, each data point in left panels in A and B represent averaged instantaneous mIPSC frequency, binned in 15 s intervals.

Gly- and GABA_AR subunit expression differed somewhat in SDH and DDH. For GlyRs, the $\alpha 1$ and β subunits dominate in both SDH and DDH, expression of the $\alpha 2$ GlyR subunit was higher in DDH, whereas $\alpha 3$ subunits were expressed equally in both regions. For GABA_ARs, $\alpha 1$ and $\beta 2$ subunit expression was higher in the DDH. In contrast to previous reports, using immunohistochemistry, we found CB₁ receptor expression to be higher in the DDH.

Contributions of glycine- and GABA_ARs in dorsal horn function

To our knowledge this study is the first comparison of Gly- and GABA_AR properties in superficial and deep laminae of the mouse spinal cord dorsal horn. Previously, we have used parasagittal slices (vs. transverse in this study) to compare Gly- and GABA_AR-mediated mIPSCs in superficial laminae (I-II) of wildtype C57/Bl6 mice and the

**Figure 5**

Effect of methanandamide on GABA_AR-mediated synaptic transmission in SDH and DDH neurons. **A** Plot showing GABA_AR-mediated mIPSC frequency (holding potential -70 mV) in an SDH neuron during bath application of methAEA (5 μm, upper bar). mIPSC frequency declines significantly in the presence of methAEA. Middle traces are averaged mIPSCs (n = 15) in control conditions and after 10 minutes in methAEA. Black bars above x-axis indicate when averaged mIPSCs were obtained. Plot on right summarizes proportional changes to GABA_AR-mediated mIPSC properties in methAEA. mIPSC frequency is reduced and rise time is slowed, however, mIPSC peak amplitude and decay time constant are not altered. **B** Effect of methAEA on GABA_AR-mediated mIPSCs in DDH neurons (presented in same format as A). methAEA significantly reduced GABA_AR-mediated mIPSC frequency, however, mIPSC peak amplitude, rise time, and decay time-constant were not altered in DDH neurons. Each data point on left panels in A and B represent averaged instantaneous mIPSC frequency, binned in 15 s intervals.

GlyR mutants *spastic* and *oscillator* [39]. As in the present study, a greater proportion of SDH neurons received GABA_AR- versus GlyR-mediated inhibition. GABA_AR- and GlyR-mediated mIPSC amplitude was also similar to that observed in wildtype mice in our previous work. In parasagittal slices, however, mIPSC frequency was higher and decay time constants were slower for both Gly- and GABA_ARs. The higher mIPSC frequency is probably due to

the rostro-caudal orientation of the dendritic trees of SDH neurons [45] as their parasagittal orientation would result in retention of more synapses in a slice. It is unclear, however, why decay time constants are slower in parasagittal slices.

Our data show that the contribution of GlyRs to fast inhibitory synaptic transmission is greater in the DDH

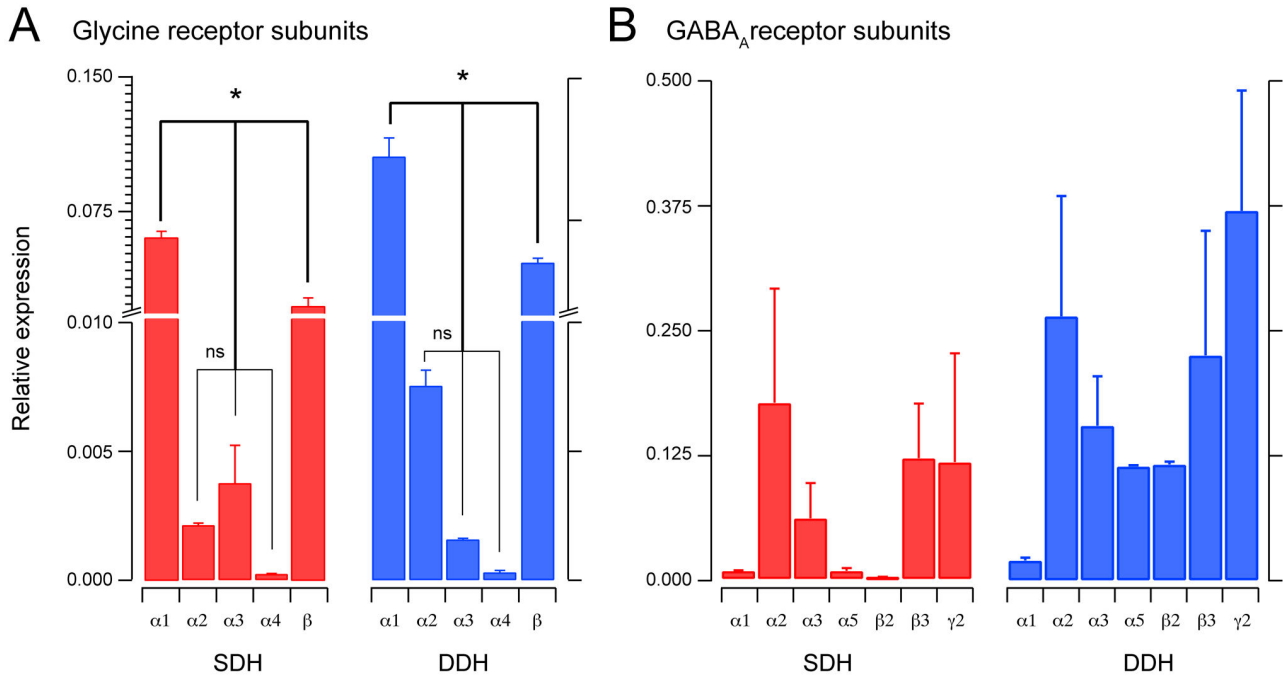


Figure 6

Gly- and GABA_A-subunit expression in the SDH and DDH. **A** plots summarising qPCR analysis for GlyR subunits. Bars represent relative expression of GlyR subunits in the SDH and DDH. The α1 and β subunits were the most highly expressed in both SDH and DDH, whereas expression of the α4 subunit was negligible. The α2 and α3 subunits were expressed at lower levels in both regions. Overall, α1, β, and α2-4 subunits were expressed at significantly different levels in both regions. Note, scale on the y-axis has been broken and expanded to facilitate comparison of subunits showing lower expression levels. **B** plots summarising qPCR analysis for GABA_AR subunits. Bars represent relative expression of GABA_AR subunits in the SDH and DDH. Overall, GABA_AR subunit expression was more variable than that observed for GlyR subunits. No significant differences in expression levels were identified, however, the expression profile for each subunit was similar in both SDH and DDH (ie, higher expression of α2, α3, β3, and γ2).

Table 2: Glycine receptor subunit expression ratio's in SDH and DDH

	Glyα1		Glyα2		Glyα3		Glyα4		Glyβ	
	SDH	DDH	SDH	DDH	SDH	DDH	SDH	DDH	SDH	DDH
Glyα1			0.04 ± 0.00	0.08 ± 0.01	0.06 ± 0.02*	0.02 ± 0.00*	0.00 ± 0.00	0.00 ± 0.00	0.39 ± 0.10	0.51 ± 0.04
Glyα2	29.1 ± 2.8*	12.6 ± 1.1*			1.8 ± 0.8*	0.20 ± 0.01*	0.12 ± 0.00*	0.05 ± 0.00*	12.5 ± 0.4*	7.6 ± 1.3*
Glyα3	21.2 ± 4.2*	63.2 ± 6.9*	0.78 ± 0.18*	5.0 ± 0.2*			0.11 ± 0.0*	0.23 ± 0.01*	18.7 ± 6.6	33.5 ± 2.8
Glyα4	252.6 ± 20.8	269.8 ± 22.0	8.7 ± 0.3*	21.4 ± 0.3*	9.1 ± 0.3*	4.3 ± 0.3*			166.2 ± 53.9	467.3 ± 3.3
Glyβ	3.7 ± 1.6	1.5 ± 0.2	0.08 ± 0.00*	0.11 ± 0.01*	0.07 ± 0.1	0.03 ± 0.00	0.01 ± 0.00	0.01 ± 0.00		

* indicates significant difference in subunit ratios between SDH and DDH

versus SDH, whereas GABA_AR-mediated inhibition appears to be equally important in both regions. In rat, Cronin et al. (2004) used c-Fos expression to functionally assess tonic inhibitory drive mediated by GlyRs and GABA_ARs in dorsal horn and suggested GlyR-mediated mechanisms are more important for setting inhibitory tone in DDH. Our data are consistent with this finding and other data for rats. For example glycine-containing neurons [46,47] and glycine terminals are more concentrated in deeper dorsal horn laminae [48]. In contrast, GABA containing neurons and terminals populate the entire dorsal horn [46,49]. Thus, our mouse data are consistent with a clear regional variation of glycinergic and GABA_Aergic inhibition in the rodent dorsal horn.

In mouse, Gly- and GABA_ARs with differing physiological properties contribute to fast synaptic inhibition in the SDH and DDH. Our data can be compared to a recent study in rat [50], even though the definition of "deep" dorsal horn varied from ours (laminae III-IV vs. laminae IV-VI). In the rat study, a greater proportion of neurons in the DDH received GlyR-mediated mIPSCs and receptor properties were similar in each region. We also found almost all neurons received GlyR-mediated mIPSCs in the mouse DDH, however, the properties of GlyRs differed markedly in SDH versus DDH. Specifically, mIPSC frequency and amplitudes were higher, and mIPSC decay times were faster in the DDH. Developmental processes may explain these differences as the rat study used younger animals (P10-15 rats vs. P17-37 mice). The importance of GABA_AR- and GlyR- mediated inhibitory processing mechanisms changes in SDH neurons during postnatal development (at least from P0-14), with glycinergic transmission maturing later [51]. Exactly when inhibitory mechanisms are functionally mature in rat is not known. In mice, however, we have shown that GlyR properties do not change in SDH neurons after P17 [39]. Moreover, SDH neurons are certainly electrically mature in the P17-37 mice used in this study [33]. It is unknown whether DDH neurons are mature by P17. Together, this work suggests significantly more GlyRs, with faster kinetics, contribute to GlyR-mediated inhibition in mouse DDH.

GlyRs in mouse SDH and DDH differ in their decay times (8-10 ms vs. 4-5 ms, respectively). The fast decay times of GlyR-mediated mIPSCs in DDH neurons (4-5 ms) match previous reports for both mice [52] and rats [53,54] for GlyRs that contain α 1 and β subunits. One potential explanation for the slower kinetics of SDH versus DDH GlyRs in mouse is the existence of a distinctly expressed type of GlyR, containing α 3 subunits, in lamina II of the mouse SDH [22]. As for other GlyRs, subunit composition (ie, Gly α 1 vs. Gly α 2) can shape channel kinetics [53,55].

This, however, does not appear to be the case for α 3 containing GlyRs in the mouse SDH as decay times, at least for evoked GlyR-mediated currents, are identical in wildtype and α 3 knockout mice [22]. One explanation is that the somato-dendritic distribution of inhibitory synapses may differ for SDH versus DDH neurons. For example, preferential localization of GlyRs on dendrites would decrease the amplitude and slow the decay time of GlyR-mediated mIPSCs [56]. Such dendritic filtering effects would, however, also slow rise times of GlyR-mediated mIPSCs and this was not the case (Table 1). Thus, future experiments are needed to determine why the kinetics of GlyR channels in the SDH and DDH differ.

In contrast to the marked difference in the contribution of GlyRs to inhibition in the SDH and DDH, GABA_AR-mediated inhibition appears equally important in both spinal cord regions. These observations are consistent with immunohistochemical data in rat showing that GABA-containing neurons, GABA positive terminals and GABA_ARs are equally distributed across the dorsal horn. The only major difference we observed in mouse dorsal horn was a slower decay time constant (23 vs. 18 ms) in SDH versus DDH neurons. The faster kinetics of mIPSCs in DDH neurons, are consistent with higher expression of the α 1 GABA_AR subunit in deeper lamina [57] as incorporation of the α 1 subunit decreases channel open time and mIPSC decay time [58,59]. Thus, in mice, GABA_AR-mediated inhibitory transmission appears equally important across the entire dorsal horn, however, GABA_ARs in the DDH have faster kinetics.

The different decay times we report for both GlyR- and GABA_AR-mediated mIPSCs in mouse SDH versus DDH point to varying subunit composition. Our qPCR data for GlyR subunits show that the balance of GlyR-subunit expression differs in SDH and DDH. Not surprisingly, the α 1 and β subunits of the GlyR, the ubiquitous adult form of the receptor [60,61], dominate in both regions. The α 2 subunit, however, is expressed at higher levels in the DDH. This can not explain the slower kinetics of SDH mIPSCs, as developmental studies in spinal cord [55] and brainstem neurons [39,53] show GlyRs containing α 2 subunits have slower kinetics. Interestingly, our qPCR data did not show higher α 3 expression in the SDH as reported by Harvey et al., (2004) using immunohistochemistry. A scenario where α 3 subunit is preferentially directed to synaptic locations in SDH, whereas in DDH the protein remains at extrasynaptic locations would explain these differences. This needs to be considered when comparing electrophysiological data, which only assesses synaptic receptors versus qPCR data which assesses subunit expression without considering location. Our qPCR data for GABA_AR subunits showed there was significantly

greater expression of GABA_A α 1 and β 2 subunits in the DDH versus the SDH. These data are consistent with reports showing GABA_ARs containing α 1 subunits have faster kinetics [58,59].

Endocannabinoid actions on fast inhibitory receptors in SDH and DDH

Our data show clearly that the endocannabinoid analogue, methAEA (5 μ M), reduces GlyR- and GABA_AR-mediated mIPSC frequency in both SDH and DDH neurons. These findings are consistent with the "in vivo" view of endocannabinoid action, whereby they are released postsynaptically and act retrogradely at presynaptic terminals to reduce neurotransmitter release [62-66]. The reduced mIPSC frequency we measured in the presence of methAEA is also consistent with immunohistochemical investigations showing that the CB₁R is expressed on the presynaptic terminals of local circuit neurons, descending inputs, as well as peripheral sensory afferents in the spinal cord [25,62,67].

The negative action of methAEA on both GlyR- and GABA_AR-mediated inhibition appears to be at odds with the well-documented antinociceptive effects of cannabinoids. In vivo administration of GlyR and GABA_AR antagonists produces hyperalgesia and tactile allodynia rather than analgesia [68,69]. These apparently conflicting observations made using in vitro and in vivo preparations emphasise that the **net effect** of cannabinoids on spinal circuits determines dorsal horn output. It is well known that cannabinoids also decrease excitatory drive in the dorsal horn, based on reduction of glutamate-mediated mEPSCs [62,70]. New information using paired recording techniques in the SDH indicates that most (~70%) of the connections within lamina II are excitatory [71]. These new data fit with the "net effect" hypothesis. Perhaps these comparisons emphasize the lack of information on specific circuits in spinal cord pain pathway and the roles of various interneuronal populations in dorsal horn function)[72].

Because two recent reports suggest cannabinoids can **directly** modulate GlyRs in isolated neurons or oocytes [31,32], we tested the effects of methAEA on GlyR-mediated mIPSCs in both SDH and DDH neurons. We found no evidence for a 'direct effect' of methAEA on GlyR function in either SDH or DDH. There are several explanations for why we did not observe a direct effect of methAEA on GlyRs. First, our study employed a more 'physiologically intact' preparation where factors such as receptor clustering, local glycine concentration and subunit composition would differ markedly. Second, recent reports suggest the direct effects of cannabinoids on recombinant GlyRs is subunit-specific, and glycine-concentration dependent [73].

We also tested for direct effects of cannabinoids on GABA_Aergic mIPSCs. In both SDH and DDH neurons methAEA reduced mIPSC frequency and did not alter mIPSC amplitude. Similar responses have been reported in the cerebellum [74]. In addition, we observed a significant effect of methAEA on GABA_AR-mediated mIPSC rise time, however, this was confined to SDH neurons. This is perhaps not surprising, as GABA_ARs are modulated by a multitude of exogenous and endogenous substances. For example, the benzodiazepines [75], gaseous and intravenous anaesthetics [76], alcohols [77], neurosteroids [78] and zinc [79] can all positively modulate the GABA_AR responses to GABA via allosteric actions on the receptor complex. Thus, cannabinoids may prove to be yet another modulatory agent of GABA_AR-mediated signaling.

Implications for spinal cord processing of sensory information

Previous work has shown that the SDH and DDH receive different types of peripheral input, project to different supraspinal targets and exhibit considerable variation in their intrinsic connectivity [18,19,71]. We propose that clear differences also exist in inhibitory control mechanisms within each region. Glycinergic signalling dominates in the DDH, whereas GABA_A signalling is equally important in both regions. Finally, there appears to be need for an inhibitory system with fast and slow kinetics *within* both superficial and deep regions of the mouse spinal cord. GlyR-mediated inhibition is more important in deep regions of the dorsal horn, which preferentially receive peripheral inputs from axons with high conduction velocities [3,12]. The existence of large and fast inhibitory inputs in the DDH would be well suited to modulate the effects of such inputs. In contrast, smaller and slower GABA_AR-mediated inhibition appears to be equally important in both superficial and deep regions of the spinal cord dorsal horn. These features suggest GABA_AR-mediated inhibition is more important for fine-tuning the effects of a functionally wider range of peripheral inputs.

Suppression of inhibitory signalling in the dorsal horn, which occurs in certain chronic pain states, can lead to hypersensitivity and tactile allodynia [68,80-82]. Both SDH and DDH neurons have been implicated in this form of plasticity, reinforcing the notion that both regions of the dorsal horn play key roles in nociception even though the SDH preferentially receives nociceptive input. The segregation of excitation and information processing in the two regions is hypothesised to play a key role in the segregation of noxious and innocuous sensory experience. The importance of both glycinergic and GABA_Aergic inhibition in this segregation was clearly illustrated in recent calcium imaging experiments in spinal cord slices [83]. In the control condition, dorsal root stimulation resulted in discrete and localized excitation that was restricted to the

SDH. When the same preparation was stimulated under conditions where inhibition was blocked, excitation spread from the SDH to DDH and even contralaterally. These findings highlight the importance of inhibitory control of cross talk between the SDH and DDH. Consequently, a greater understanding of the properties of inhibitory mechanisms in the two regions will help identify new strategies for treating nociceptive dysfunction in the spinal cord dorsal horn.

Competing interests

The authors declare that they have no competing interests.

Authors' contributions

WBA and BAG participated equally in the experimental design, performing experiments, analysis and manuscript preparation. NJB and PAT performed and analyzed the qPCR experiments. The work was carried out in the laboratories of AMB and RJC who contributed to experimental design, analysis and manuscript preparation. All authors have read and approved the final version of the manuscript.

Additional material

Additional file 1

Primer sequences for PCR analysis. Table showing primer sequences for PCR analysis.

Click here for file

[<http://www.biomedcentral.com/content/supplementary/1744-8069-5-65-S1.DOC>]

Acknowledgements

This work was supported by the National Health and Medical Research Council of Australia (Grants 276403, 401244 and 569206), The Hunter Medical Research Institute, and the University of Newcastle, Australia.

References

- Willis WD, Coggeshall RE: *Sensory Mechanisms of the Spinal Cord* 3rd edition. New York: Kluwer Academic/Plenum Publishers; 2004.
- Todd AJ, Koerber HR: **Neuroanatomical substrates of spinal nociception.** In *Wall and Melzack's Textbook of Pain* 5th edition. Edited by: McMahon SB, Koltzenburg M. Philadelphia: Elsevier Churchill Livingstone; 2006:73-90.
- Brown AG: **The dorsal horn of the spinal cord.** *Q J Exp Physiol* 1982, **67**:193-212.
- Light AR, Perl ER: **Re-examination of the dorsal root projection to the spinal dorsal horn including observations on the differential termination of coarse and fine fibers.** *J Comp Neurol* 1979, **186**:117-131.
- Light AR, Perl ER: **Spinal termination of functionally identified primary afferent neurons with slowly conducting myelinated fibers.** *J Comp Neurol* 1979, **186**:133-150.
- Christensen BN, Perl ER: **Spinal neurons specifically excited by noxious or thermal stimuli: marginal zone of the dorsal horn.** *J Neurophysiol* 1970, **33**:293-307.
- Sugiura Y, Lee CL, Perl ER: **Central projections of identified, unmyelinated (C) afferent fibers innervating mammalian skin.** *Science* 1986, **234**:358-361.
- Tuckett RP, Wei JY: **Response to an itch-producing substance in cat. I. Cutaneous receptor populations with myelinated axons.** *Brain Res* 1987, **413**:87-94.
- Tuckett RP, Wei JY: **Response to an itch-producing substance in cat. II. Cutaneous receptor populations with unmyelinated axons.** *Brain Res* 1987, **413**:95-103.
- Vallbo AB, Olausson H, Wessberg J: **Unmyelinated afferents constitute a second system coding tactile stimuli of the human hairy skin.** *J Neurophysiol* 1999, **81**:2753-2763.
- Koerber HR, Woodbury CJ: **Comprehensive phenotyping of sensory neurons using an ex vivo somatosensory system.** *Physiol Behav* 2002, **77**:589-594.
- Koerber HR, Brown PB: **Quantitative analysis of dorsal horn cell receptive fields following limited deafferentation.** *J Neurophysiol* 1995, **74**:2065-2076.
- Woolf CJ: **Central terminations of cutaneous mechanoreceptive afferents in the rat lumbar spinal cord.** *J Comp Neurol* 1987, **261**:105-119.
- Craig ADB: **Pain mechanisms: labeled lines versus convergence in central processing.** *Ann Rev Neurosci* 2003, **26**:1-30.
- Klop EM, Mouton LJ, Hulsebosch R, Boers J, Holstege G: **In cat four times as many lamina I neurons project to the parabrachial nuclei and twice as many to the periaqueductal gray as to the thalamus.** *Neuroscience* 2005, **134**:189-197.
- Kobayashi Y: **Distribution and morphology of spinothalamic tract neurons in the rat.** *Anat Embryol (Berl)* 1998, **197**:51-67.
- Willis WD Jr, Zhang X, Honda CN, Giesler GJ Jr: **Projections from the marginal zone and deep dorsal horn to the ventrobasal nuclei of the primate thalamus.** *Pain* 2001, **92**:267-276.
- Lu Y, Perl ER: **A Specific inhibitory pathway between substantia gelatinosa neurons receiving direct C-fiber input.** *J Neurosci* 2003, **23**:8752-8758.
- Lu Y, Perl ER: **Modular organization of excitatory circuits between neurons of the spinal superficial dorsal horn (laminae I and II).** *J Neurosci* 2005, **25**:3900-3907.
- Schneider SP: **Local circuit connections between hamster laminae III and IV dorsal horn neurons.** *J Neurophysiol* 2008, **99**:1306-1318.
- Cronin JN, Bradbury EJ, Lidieth M: **Laminar distribution of GABAA- and glycine-receptor mediated tonic inhibition in the dorsal horn of the rat lumbar spinal cord: effects of picrotoxin and strychnine on expression of Fos-like immunoreactivity.** *Pain* 2004, **112**:156-163.
- Harvey RJ, Depner UB, Wassle H, Ahmadi S, Heindl C, Reinold H, Smart TG, Harvey K, Schutz B, Abo-Salem OM, Zimmer A, Poisbeau P, Welzl H, Wolfer DP, Betz H, Zeilhofer HU, Muller U: **GlyR alpha3: an essential target for spinal PGE2-mediated inflammatory pain sensitization.** *Science* 2004, **304**:884-887.
- Gilbert PE: **A comparison of THC, nandrolone, and morphine in the chronic spinal dog.** *J Clin Pharmacol* 1981, **21**:311S-319S.
- Smith PB, Martin BR: **Spinal mechanisms of delta 9-tetrahydrocannabinol-induced analgesia.** *Brain Res* 1992, **578**:8-12.
- Farquhar-Smith WP, Egertova M, Bradbury EJ, McMahon SB, Rice AS, Elphick MR: **Cannabinoid CB(1) receptor expression in rat spinal cord.** *Mol Cell Neurosci* 2000, **15**:510-521.
- Richardson JD, Aanonsen L, Hargreaves KM: **Hypoactivity of the spinal cannabinoid system results in NMDA-dependent hyperalgesia.** *J Neurosci* 1998, **18**:451-457.
- Shen M, Piser TM, Seybold VS, Thayer SA: **Cannabinoid receptor agonists inhibit glutamatergic synaptic transmission in rat hippocampal cultures.** *J Neurosci* 1996, **16**:4322-4334.
- Lichtman AH, Martin BR: **Cannabinoid-induced antinociception is mediated by a spinal alpha 2-noradrenergic mechanism.** *Brain Res* 1991, **559**:309-314.
- Pugh G Jr, Smith PB, Dombrowski DS, Welch SP: **The role of endogenous opioids in enhancing the antinociception produced by the combination of delta 9-tetrahydrocannabinol and morphine in the spinal cord.** *J Pharmacol Exp Ther* 1996, **279**:608-616.
- Reche I, Fuentes JA, Ruiz-Gayo M: **A role for central cannabinoid and opioid systems in peripheral delta 9-tetrahydrocannabinol-induced analgesia in mice.** *Eur J Pharmacol* 1996, **301**:75-81.
- Hejazi N, Zhou C, Oz M, Sun H, Ye JH, Zhang L: **Delta9-tetrahydrocannabinol and endogenous cannabinoid anandamide**

- directly potentiate the function of glycine receptors. *Mol Pharmacol* 2006, **69**:991-997.
32. Lozovaya N, Yatsenko N, Beketov A, Tsintsadze T, Burnashev N: **Glycine receptors in CNS neurons as a target for nonretrograde action of cannabinoids.** *J Neurosci* 2005, **25**:7499-7506.
 33. Walsh MA, Graham BA, Brichta AM, Callister RJ: **Evidence for a critical period in the development of excitability and potassium currents in mouse lumbar superficial dorsal horn neurons.** *J Neurophysiol* 2009, **101**:1800-1812.
 34. Bekkers JM, Stevens CF: **NMDA and non-NMDA receptors are co-localized at individual excitatory synapses in cultured rat hippocampus.** *Nature* 1989, **341**:230-233.
 35. Graham BA, Brichta AM, Schofield PR, Callister RJ: **Altered potassium channel function in the superficial dorsal horn of the spastic mouse.** *J Physiol (Lond)* 2007, **584**:121-136.
 36. Franklin KBJ, Paxinos G: *Mouse Brain in Stereotaxic Coordinates* 3rd edition. San Deigo: Academic Press; 1997.
 37. Clements JD, Bekkers JM: **Detection of spontaneous synaptic events with an optimally scaled template.** *Biophys J* 1997, **73**:220-229.
 38. Callister RJ, Walmsley B: **Amplitude and time course of evoked and spontaneous synaptic currents in rat submandibular ganglion cells.** *J Physiol (Lond)* 1996, **490**:149-157.
 39. Graham BA, Schofield PR, Sah P, Callister RJ: **Altered inhibitory synaptic transmission in superficial dorsal horn neurones in spastic and oscillator mice.** *J Physiol (Lond)* 2003, **551**:905-916.
 40. Traynelis SF, Silver RA, Cull-Candy SG: **Estimated conductance of glutamate receptor channels activated during EPSCs at the cerebellar mossy fiber-granule cell synapse.** *Neuron* 1993, **11**:279-289.
 41. Beveridge NJ, Tooney PA, Carroll AP, Gardiner E, Bowden N, Scott RJ, Tran N, Dedova I, Cairns MJ: **Dysregulation of miRNA 181b in the temporal cortex in schizophrenia.** *Hum Mol Genet* 2008, **17**:1156-1168.
 42. Molander C, Xu Q, Grant G: **The cytoarchitectonic organization of the spinal cord in the rat. I. The lower thoracic and lumbosacral cord.** *J Comp Neurol* 1984, **230**:133-141.
 43. Rexed B: **The cytoarchitectonic organization of the spinal cord in the cat.** *J Comp Neurol* 1952, **96**:414-495.
 44. Lozovaya N, Yatsenko N, Beketov A, Tsintsadze T, Burnashev N: **Glycine Receptors in CNS Neurons as a Target for Nonretrograde Action of Cannabinoids.** *J Neurosci* 2005, **25**:7499-7506.
 45. Chery N, Yu XH, de Koninck Y: **Visualization of lamina I of the dorsal horn in live adult rat spinal cord slices.** *J Neurosci Methods* 2000, **96**:133-142.
 46. Todd AJ, Sullivan AC: **Light microscope study of the coexistence of GABA-like and glycine-like immunoreactivities in the spinal cord of the rat.** *J Comp Neurol* 1990, **296**:496-505.
 47. Zeilhofer HU, Studler B, Arabadzisz D, Schweizer C, Ahmadi S, Layh B, Bosl MR, Fritschy JM: **Glycinergic neurons expressing enhanced green fluorescent protein in bacterial artificial chromosome transgenic mice.** *J Comp Neurol* 2005, **482**:123-141.
 48. Zeilhofer HU: **The glycinergic control of spinal pain processing.** *Cell Mol Life Sci* 2005, **62**:2027-2035.
 49. Mackie M, Hughes DI, Maxwell DJ, Tillakaratne NJ, Todd AJ: **Distribution and colocalisation of glutamate decarboxylase isoforms in the rat spinal cord.** *Neuroscience* 2003, **119**:461-472.
 50. Inquimbert P, Rodeau JL, Schlichter R: **Differential contribution of GABAergic and glycinergic components to inhibitory synaptic transmission in lamina II and laminae III-IV of the young rat spinal cord.** *Eur J Neurosci* 2007, **26**:2940-2949.
 51. Baccei ML, Fitzgerald M: **Development of GABAergic and Glycinergic Transmission in the Neonatal Rat Dorsal Horn.** *J Neurosci* 2004, **24**:4749-4757.
 52. Graham BA, Schofield PR, Sah P, Margrie TW, Callister RJ: **Distinct Physiological Mechanisms Underlie Altered Glycinergic Synaptic Transmission in the Murine Mutants spastic, spasmodic, and oscillator.** *J Neurosci* 2006, **26**:4880-4890.
 53. Singer JH, Talley EM, Bayliss DA, Berger AJ: **Development of glycinergic synaptic transmission to rat brain stem motoneurons.** *J Neurophysiol* 1998, **80**:2608-2620.
 54. Chery N, de Koninck Y: **Junctional versus extrajunctional glycine and GABA(A) receptor-mediated IPSCs in identified lamina I neurons of the adult rat spinal cord.** *J Neurosci* 1999, **19**:7342-7355.
 55. Takahashi T, Momiyama A: **Single-channel currents underlying glycinergic inhibitory postsynaptic responses in spinal neurons.** *Neuron* 1991, **7**:965-969.
 56. Lim R, Alvarez FJ, Walmsley B: **Quantal size is correlated with receptor cluster area at glycinergic synapses in the rat brainstem.** *J Physiol (Lond)* 1999, **516**(Pt 2):505-512.
 57. Bohlhalter S, Weinmann O, Mohler H, Fritschy J: **Laminar compartmentalization of GABAA-receptor subtypes in the spinal cord: an immunohistochemical study.** *J Neurosci* 1996, **16**:283-297.
 58. Bosman LW, Heinen K, Spijker S, Brussaard AB: **Mice lacking the major adult GABAA receptor subtype have normal number of synapses, but retain juvenile IPSC kinetics until adulthood.** *J Neurophysiol* 2005, **94**:338-346.
 59. Brussaard AB, Kits KS, Baker RE, Willems WP, Leyting-Vermeulen JW, Voorn P, Smit AB, Bicknell RJ, Herbinson AE: **Plasticity in fast synaptic inhibition of adult oxytocin neurons caused by switch in GABA(A) receptor subunit expression.** *Neuron* 1997, **19**:1103-1114.
 60. Legendre P: **The glycinergic inhibitory synapse.** *Cell Mol Life Sci* 2001, **58**:760-793.
 61. Lynch JW: **Molecular structure and function of the glycine receptor chloride channel.** *Physiol Rev* 2004, **84**:1051-1095.
 62. Morrisset V, Urban L: **Cannabinoid-induced presynaptic inhibition of glutamatergic EPSCs in substantia gelatinosa neurons of the rat spinal cord.** *J Neurophysiol* 2001, **86**:40-48.
 63. Twitchell W, Brown S, Mackie K: **Cannabinoids inhibit N- and P/Q-type calcium channels in cultured rat hippocampal neurons.** *J Neurophysiol* 1997, **78**:43-50.
 64. Katona I, Sperlagh B, Sik A, Kafalvi A, Vizi ES, Mackie K, Freund TF: **Presynaptically located CB1 cannabinoid receptors regulate GABA release from axon terminals of specific hippocampal interneurons.** *J Neurosci* 1999, **19**:4544-4558.
 65. Schlicker E, Kathmann M: **Modulation of transmitter release via presynaptic cannabinoid receptors.** *Trends Pharmacol Sci* 2001, **22**:565-572.
 66. Vaughan CW, Christie MJ: **Retrograde signalling by endocannabinoids.** *Handb Exp Pharmacol* 2005:367-383.
 67. Salio C, Fischer J, Franzoni MF, Conrath M: **Pre- and postsynaptic localizations of the CB1 cannabinoid receptor in the dorsal horn of the rat spinal cord.** *Neuroscience* 2002, **110**:755-764.
 68. Yaksh TL: **Behavioral and autonomic correlates of the tactile evoked allodynia produced by spinal glycine inhibition: effects of modulatory receptor systems and excitatory amino acid antagonists.** *Pain* 1989, **37**:111-123.
 69. Sivilotti L, Woolf CJ: **The contribution of GABAA and glycine receptors to central sensitization: disinhibition and touch-evoked allodynia in the spinal cord.** *J Neurophysiol* 1994, **72**:169-179.
 70. Jennings EA, Vaughan CW, Roberts LA, Christie MJ: **The actions of anandamide on rat superficial medullary dorsal horn neurons in vitro.** *J Physiol (Lond)* 2003, **548**:121-129.
 71. Santos SFA, Rebelo S, Derkach VA, Sazonov BV: **Excitatory interneurons dominate sensory processing in the spinal substantia gelatinosa of rat.** *J Physiol (Lond)* 2007, **581**:241-254.
 72. Graham BA, Brichta AM, Callister RJ: **Moving from an averaged to specific view of spinal cord pain processing circuits.** *J Neurophysiol* 2007, **98**:1057-1063.
 73. Yang Z, Aubrey KR, Alroy I, Harvey RJ, Vandenberg RJ, Lynch JW: **Subunit-specific modulation of glycine receptors by cannabinoids and N-arachidonyl-glycine.** *Biochem Pharmacol* 2008, **76**:1014-1023.
 74. Diana MA, Levenes C, Mackie K, Marty A: **Short-term retrograde inhibition of GABAergic synaptic currents in rat Purkinje cells is mediated by endogenous cannabinoids.** *J Neurosci* 2002, **22**:200-208.
 75. Haefely W, Kulcsar A, Mohler H, Pieri L, Polc P, Schaffner R: **Possible involvement of GABA in the central actions of benzodiazepines.** *Adv Biochem Psychopharmacol* 1975:131-151.
 76. Lin LH, Whiting P, Harris RA: **Molecular determinants of general anesthetic action: role of GABAA receptor structure.** *J Neurochem* 1993, **60**:1548-1553.
 77. Soldo BL, Proctor WR, Dunwiddie TV: **Ethanol differentially modulates GABAA receptor-mediated chloride currents in hippocampal, cortical, and septal neurons in rat brain slices.** *Synapse* 1994, **18**:94-103.

78. Belelli D, Lambert JJ: **Neurosteroids: endogenous regulators of the GABA(A) receptor.** *Nat Rev Neurosci* 2005, **6**:565-575.
79. Hosie AM, Dunne EL, Harvey RJ, Smart TG: **Zinc-mediated inhibition of GABA(A) receptors: discrete binding sites underlie subtype specificity.** *Nat Neurosci* 2003, **6**:362-369.
80. Sivilotti L, Woolf CJ: **The contribution of GABA(A) and glycine receptors to central sensitization: disinhibition and touch-evoked allodynia in the spinal cord.** *J Neurophysiol* 1994, **72**:169-179.
81. Kontinen VK, Stanfa LC, Basu A, Dickenson AH: **Electrophysiologic evidence for increased endogenous gabaergic but not glycinergic inhibitory tone in the rat spinal nerve ligation model of neuropathy.** *Anesthesiology* 2001, **94**:333-339.
82. Moore KA, Kohno T, Karchewski LA, Scholz J, Baba H, Woolf CJ: **Partial peripheral nerve injury promotes a selective loss of GABAergic inhibition in the superficial dorsal horn of the spinal cord.** *J Neurosci* 2002, **22**:6724-6731.
83. Ruscheweyh R, Sandkuhler J: **Long-range oscillatory Ca²⁺ waves in rat spinal dorsal horn.** *Eur J Neurosci* 2005, **22**:1967-1976.

Publish with **BioMed Central** and every scientist can read your work free of charge

"BioMed Central will be the most significant development for disseminating the results of biomedical research in our lifetime."

Sir Paul Nurse, Cancer Research UK

Your research papers will be:

- available free of charge to the entire biomedical community
- peer reviewed and published immediately upon acceptance
- cited in PubMed and archived on PubMed Central
- yours — you keep the copyright

Submit your manuscript here:
http://www.biomedcentral.com/info/publishing_adv.asp

